

# Coaxial Injection Mixer for the Continuous Production of Nanoparticles

Diego Caccavo<sup>a,\*</sup>, Gaetano Lamberti<sup>a</sup>, Anna Angela Barba<sup>b</sup>

<sup>a</sup> Department of Industrial Engineering, University of Salerno, Fisciano (SA), via Giovanni Paolo II 132, 84084, Italy

<sup>b</sup> Department of Pharmacy, University of Salerno, Fisciano (SA), via Giovanni Paolo II 132, 84084, Italy;  
 dcaccavo@unisa.it

Nanoparticles (NPs) production in batch reactors is limited in terms of reproducibility and control over physical properties such as particle size. Microfluidic techniques and flow-focusing can improve these limitations, but continuous nanoprecipitation through turbulent mixing can also be achieved. This study evaluates the effect of fluid dynamics on NP production and characteristics in a coaxial jet mixer. The results showed that the vertical and horizontal configurations of the mixer impact mixing performance, with buoyancy in the horizontal configuration causing fluid segregation and altering the coaxiality. The mixing performance was tested using water/water and ethanol/water systems with different flow rates, and results indicated that a turbulent jet develops at high values of both the Flow Momentum Ratio ( $FMR$ ) and Reynolds number ( $N_{Re}$ ). The mixing time for the turbulent jet was found to have a clear relationship with the Reynolds number and  $FMR$  and was successfully fitted using a power law equation. Finally, the results showed that the NPs produced in turbulence were smaller and more uniform in size, with a Z-average half that of those produced in laminar conditions. The improved size uniformity and reduced dimensions of the particles resulted in a clearer final product. This study suggests that micromixing is a more favourable method for producing liposomes with improved characteristics and higher productivity compared to interdiffusion.

## 1. Introduction

Nanomaterials have garnered significant attention due to their potential to generate novel and cutting-edge products across a wide range of fields. Batch type reactors are traditionally used to produce nanoparticles (NPs), however, these bulk synthesis methods can have challenges in terms of reproducibility and control over the physical and chemical properties of the NPs from one batch to another (Murday et al., 2009).

Various new technologies based on microfluidic technique and microfluidic-like (simil-microfluidic) technique have been developed to overcome these limits (Has & Sunthar, 2020). The "simil-microfluidic" approach has gained attention for its potential for high productivity, with respect to "pure" microfluidic. This method involves bringing two fluids, one in which the desired substance is soluble and the other in which it is not, into contact within a tubular device by the flow-focusing method (Bochicchio et al., 2020). Interdiffusion within these two fluids can lead to the formation of nanoparticles (Carugo et al., 2016). However, nanoprecipitation based on the simil-microfluidic approach (laminar flow regimes and interdiffusion phenomena) may not be the only possible choice to produce nanoparticles in continuous manner.

Lim et al. (Lim et al., 2014) and Saad and Prud'homme (Saad & Prud'homme, 2016) have demonstrated that continuous nanoprecipitation can also be achieved through turbulent regimes, using respectively a Coaxial Jet Mixer (CJM) and a Confined Impinging Jets (CIJ) mixer of similar size to the "simil-microfluidic" apparatus of Bochicchio et al. (Bochicchio et al., 2020). In such application the nanoprecipitation is governed by micromixing (microscopic mixing), which is the mixing that occurs at the smallest scales of motion, the Kolmogorov scale, and at the final scales of molecular diffusivity, the Batchelor scale (Paul et al., 2004). Micromixing can also be achieved in laminar macroscopic flow with static mixers, but the mixing efficiency is lower than in turbulent macroscopic flow. The high eddy diffusion in turbulent flow leads to faster mixing due to the rapid interchange of fluid positions and high shear rates that enhance mixing by disrupting interfaces and creating new areas for

diffusion (Paul et al., 2004). Micromixing is crucial in reactions, as it occurs on a small scale and accelerates reaction progress by rapidly increasing the available interfacial area for diffusion. When the micromixing time ( $\tau_m$ ) is of the same order of magnitude of the reaction time ( $\tau_r$ ), mixing becomes a critical factor affecting reaction rate, yield, and selectivity. The mixing Damköhler number ( $Da = \tau_m/\tau_r$ ) assesses the importance of mixing relative to reaction time (Gobert et al., 2017; Rehage & Kind, 2021). If the Damköhler number is low ( $<0.02$ ), mixing is faster than reaction and the reactor is well-mixed, allowing a homogenous reaction kinetic. If high ( $>100$ ), reaction is faster than mixing, so modifying mixing time affects outcome. For intermediate Damköhler numbers, both mixing and kinetics impact reaction. (Paul et al., 2004). Despite the impact of micromixing has been extensively studied in literature for chemical reactions (Bałdyga & Bourne, 1999), the same considerations can be applied to physical phenomena, such as precipitation, by replacing the reaction characteristic time with the characteristic time of the physical phenomenon, i.e. replacing the reaction time with the time of nucleation plus growth  $\tau_{n+g}$  (Saad & Prud'homme, 2016).

Optimizing nanoparticle production requires comprehensive knowledge of mixer performance, whether in laminar conditions via interdiffusion or in turbulent conditions through micromixing. This study aims to assess the influence of fluid dynamic regimes on the mixing performance and on the nanoparticle production and characteristics in a coaxial injection mixer, similar in design to the mixer of Bochicchio et al. (2020) and Lim et al. (2014). The use of the same mixer to produce nanoparticles in both laminar and turbulent regimes was never reported in literature, which would make easier to assess the impact of the phenomenology on the final characteristic of the product.

## 2. Materials and Methods

Soy-lecithin (EMULPUR® IP from Cargill, ACEF spa, Italy), as source of phospholipids to form liposomes, were bought from Bodanchimica Srl (Italy). Ethanol absolute (CAS 64-17-5), as solvent for lecithin, and Eriochrome® Black T (CAS 1787-61-7), used as tracer, were bought from Merk Life Science Srl (Italy).

### 2.1 Coaxial Injection Mixer

The system has four main components: the support, pipes, pumps, and video module. The support is made of Aluminium square tubes (Combitech® system) bought from Alfer® aluminium Gesellschaft mbH (Germany).

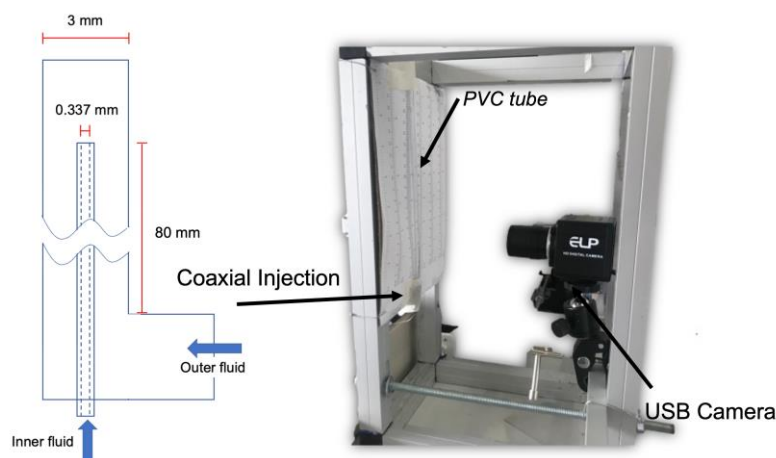


Figure 1. The Coaxial Injection Mixer used in this work.

The experimental setup comprises a vertical coaxial tube with a metric scale for image analysis and a CMOS USB Camera (ELP-USB4K03-SFV) with a 2.8-12 mm wide-angle lens. The coaxial injection system consists of a T-connector connecting two PVC tubes of 3 mm inner diameter at its two sides, and at the third end, a BD Quincke Spinal Needle 23G (with a total length of 90mm) is attached. This configuration is depicted in Figure 1. The inner fluid was pumped with a commercial syringe pump (Sono-Tek 12-05126 Dual Syringe Pump), whereas, due to the higher flow rate, the outer fluid was pumped with a continuous push-pull syringe pump to have a pulsation free flow rate (Iannone et al., 2022).

### 2.2 Characteristic parameters of the coaxial injection mixer

The fluid dynamics in the coaxial injection mixer is characterized by two dimensionless parameters: the Flow Velocity Ratio ( $FVR$ ) and the Average Reynolds Number ( $N_{Re}$ ) (Lim et al., 2014). A more comprehensive

approach could be the use of the Flow Momentum Ratio (*FMR*) instead of *FVR*, which defines the relative momentum of the inner fluid with respect to the outer fluid and is expressed as:

$$FMR = \frac{\rho_i u_i}{\rho_o u_o} \quad (1)$$

where  $\rho_i u_i$  and  $\rho_o u_o$  are the momentum ( $\rho$  is the density and  $u$  is the velocity) of the inner and outer fluid streams, respectively. The velocities are related to the volumetric flow rates of the inner and outer streams ( $Q_i$  and  $Q_o$ ) by the following equations:

$$u_i = \frac{4Q_i}{\pi d_i^2} \quad (2)$$

$$u_o = \frac{4Q_o}{\pi(D^2 - d_o^2)} \quad (3)$$

where  $d_i$  and  $d_o$  are the inner and outer diameters of the syringe needle, respectively.  $D$  is the internal diameter of the PVC pipe. The Average Reynolds Number ( $N_{Re}$ ) captures the relative influence of fluid inertia and viscous forces and is expressed as:

$$N_{Re} = \frac{Q_{mix} D}{\frac{\pi D^2}{4} v_{mix}} \quad (4)$$

Where  $Q_{mix}$  is the total volumetric flow rate and  $v_{mix}$  is the kinematic viscosity of the mixture. When dealing with non-ideal system, such as water and ethanol, the excess volume of mixing should be accounted. In this work the total volumetric flow rate was obtained from the total mass flow rate times the density of the mixture.

Whereas the *FMR* and the  $N_{Re}$  can be chosen a priori, an estimation of the micromixing time ( $\tau_m$ ) in this mixer can be obtained from the experiments, as in Lim et al. (2014):

$$\tau_m = \frac{L_{mix}}{\frac{Q_{mix}}{\frac{\pi D^2}{4}}} = \frac{L_{mix}}{\langle v_{mix} \rangle} \quad (5)$$

Where  $L_{mix}$  is the length at which the inner fluid is completely mixed with the outer fluid, i.e the tracer is spread on all the cross-sectional area of the external tube. The value of  $L_{mix}$  can be taken from image analysis.

### 2.3 Nanoparticles production

Liposome production was conducted under two distinct fluid dynamic conditions, namely laminar and turbulent. The internal fluid was a suspension constituted by lecithin in pure ethanol at 50 mg/mL, the external solution was deionized water. The Flow Momentum Ratio (*FMR* or equivalently the *FVR*) was kept constant in both conditions to ensure that the ratio of inner and outer flow rates remained equal, resulting in the same composition for the final product macroscopically. The ratio of the volumetric flow rate  $Q_i/Q_o$  was kept to 1:10, as reported in Bochicchio et al. (2020), that results in an *FMR* of 5.9 (*FVR* = 7.5). The laminar production was performed with  $Q_i=4.5$  mL/min and  $Q_o=45$  mL/min, with a  $N_{Re}=240$ . The turbulent production was performed with  $Q_i=36$  mL/min and  $Q_o=360$  mL/min, with a  $N_{Re}=1917$ .

### 2.4 Nanoparticles characterization

The produced nanosuspension was analyzed by a nephelometer (Turbidity Meter PCE-TUM 20, PCE Italia SrL), to assess the turbidity of the systems, and by a Zetasizer Nano ZS (Malvern Panalytical Ltd), based on the dynamic light scattering, to measure the dimension of the liposomes.

## 3. Results and discussion

### 3.1 Vertical vs Horizontal configuration of the Coaxial Injection Mixer

The coaxial injection mixer has potential for producing a range of nanoparticles through the nanoprecipitation process, where the solvent fluid (inner fluid) typically has a different density compared to the antisolvent fluid (outer fluid). The difference in density between the solvent and antisolvent fluids in a coaxial injection mixer can result in buoyancy, causing segregation of the fluids and altering the coaxiality, particularly affecting the flow focusing on the case of laminar production. In Figure 2 the segregation phenomenon is reported, showing the top (Figure 2.a) and the side (Figure 2.b) views of the Coaxial Injection Mixer build with a 23G needle and a PVC tube of 3 mm ID. The flow visualization in Figure 2 shows that when water is flowed at a rate of 45 mL/min

in the PVC tube, the pure ethanol plus tracer (Eriochrome® Black T) at a rate of 4.5 mL/min becomes segregated in the upper part of the PVC tube.

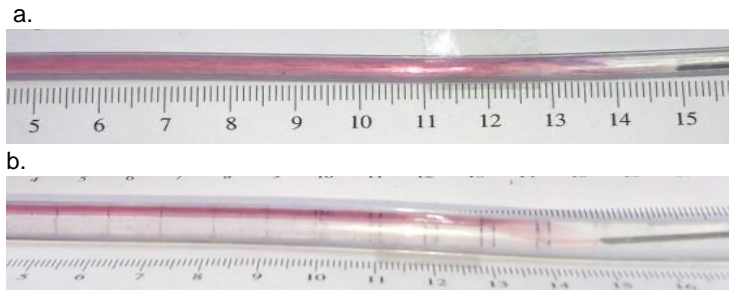


Figure 2.a. Top view and b. side view of the coaxial injection mixer in horizontal configuration. Inner fluid, pure ethanol with Eriochrome® Black T as tracer, segregation on the top part of the external tube due to buoyancy when coaxially injected in a water stream in horizontal configuration.

The system, which has a  $FMR$  of 5.9 and an average Reynolds Number ( $N_{Re}$ ) of 240, in the vertical configuration of the coaxial injection mixer (flow from bottom to top), demonstrates ideal flow focusing behavior, indicating its laminar nature. Therefore, in the design and realization of coaxial injection mixers the vertical configuration should be preferred.

### 3.2 Mixing performance of the coaxial injection mixer

The coaxial injection mixer was tested in terms of mixing performance using a water/water system and an ethanol/water system, varying the flow rates from 0.12 to 36 mL/min for the inner flow rate and from 16 to 360 mL/min for the outer flow, obtaining different values of  $N_{Re}$  and  $FMR$ . In Figure 3a and 3b, the phase diagrams generated from the flow experiments using the tracer and image analysis are presented. The working zones of laminar conditions, characterized by parallel streamlines, absence of cross-currents perpendicular to the direction of flow, and no fluid eddies or swirls, were identified and reported with red x symbol (and red area). These conditions resulted in the orderly flow of the tracer in the center of the tube, conforming to the flow-focusing requirements. In Figure 3a and 3b, the transition zone is indicated by green circles (and green area) and it is characterized by an unstable flow. Eddy formations are observed, disrupting the laminarity, however, a statistically stationary turbulence is not present. Turbulent jet conditions, in which the velocity and flow patterns do not change over time, and the jet maintain a consistent, unchanging form, were individuated and reported with blue diamond (and blue area) in Figure 3a and 3b.

As demonstrated in Figure 3a and 3b, the development of a turbulent jet occurs at high values of both Flow Momentum Ratio ( $FMR$ ) and Reynolds number ( $N_{Re}$ ). A notable difference between the two diagrams, one obtained with the water-water system (Figure 3a) and one obtained with the ethanol-water system (Figure 3b), is the extent of the transition zone, which is more pronounced in the latter. This can be attributed to the non-ideal mixing of the two fluids, resulting in a significant change in the density and viscosity of the mixture, which in turn destabilizes the laminarity of the system. Furthermore, it is observed that higher  $N_{Re}$  values are required for the ethanol-water system to produce a stable jet compared to the water-water system. This finding is in agreement with the computational results of Usta et al. (Usta et al., 2023), who reported that the formation of a turbulent jet becomes increasingly difficult as the overall viscosity increases, with lack of dispersion and turbulent diffusion. In Figure 3c the mixing time for the turbulent jet, calculated according to the equation 5, is reported against the Reynolds number ( $N_{Re}$ ) for different values of the Flow Momentum Ratio ( $FMR$ ). The circular and square symbols have been used to indicate the experiments with water/water and ethanol/water systems, respectively. Contrary to the findings of Lim et al. (2014), who reported a mixing time that was dependent only on the Reynolds number ( $N_{Re}$ ), this study demonstrates a clear relationship between mixing time and both the Reynolds number and the Flow Momentum Ratio ( $FMR$ ). The experimental data were successfully fitted using a power law equation, enabling the alteration of the pre-factors and power (which was kept constants for all experiments). The varying pre-factors were then fitted against the Flow Momentum Ratio ( $FMR$ ) and demonstrated a linear relationship. The final form of the equation that relates the mixing time to the  $FMR$  and  $N_{Re}$  is the equation 6.

$$\tau_m = (-1.48 \times 10^8 \times FMR + 1.459 \times 10^9) \times N_{Re}^{-2.22} \quad (6)$$

This power law equation was used to fit the experimental data, which produced a satisfactorily accurate representation of the experimental results, as demonstrated by the lines in Figure 3c.

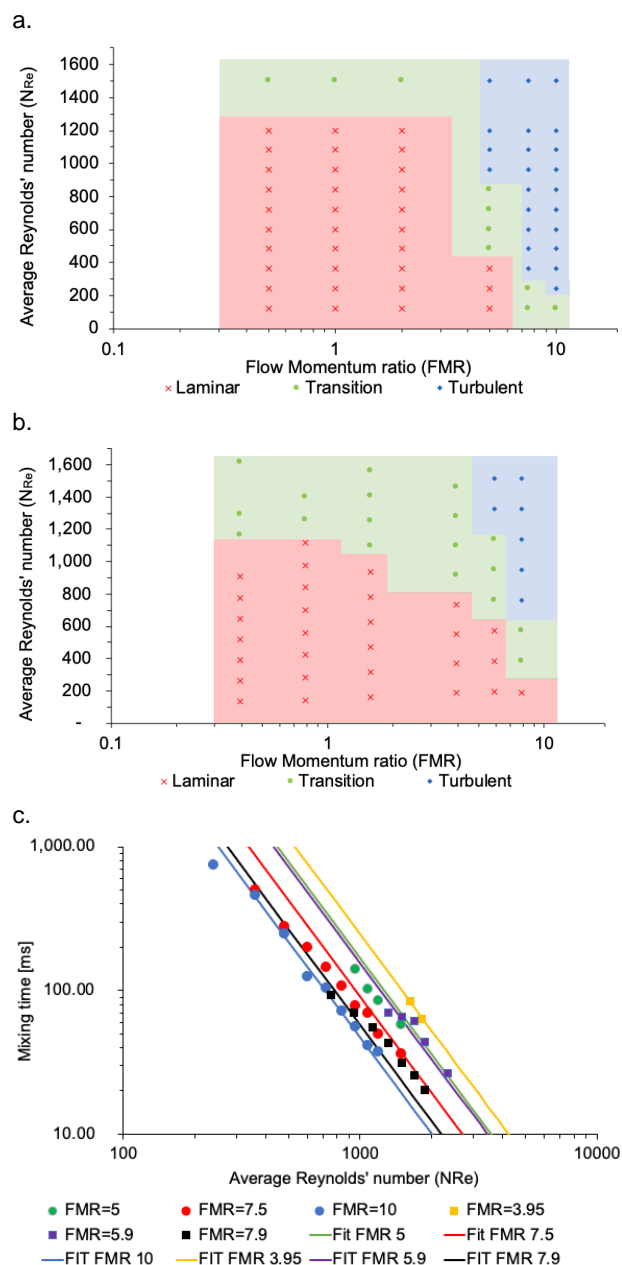


Figure 3.a. Phase diagram, in terms of FMR and  $N_{Re}$ , for water/water mixing. b. Phase diagram, in terms of FMR and  $N_{Re}$ , for pure ethanol/water mixing. c. Mixing time versus the Reynolds number for varying Flow Momentum Ratios (FMR) for the turbulent regime. The data obtained from the water-water and ethanol-water systems are represented by circular and square symbols, respectively. Straight lines indicate the fitted equation that describes the mixing time as a function of Reynolds number and FMR

### 3.3 Impact of the fluid dynamic conditions on nanoparticles characteristics

The nanoparticles produced in laminar and turbulent regime, to have the same macroscopic composition, were characterized by the nephelometer and the DLS technique, as reported in section 2. The results are reported in Table 1 in terms of Z-average, polydispersity index (PDI) and turbidity. As shown in Table 1, the Z-average, which represents the weight-average hydrodynamic diameter of the particles, indicates that the nanoparticles produced by the turbulent jet (micromixing) are substantially smaller than those formed in laminar (interdiffusion) conditions, with a Z-average value that is half of that in the laminar production. Also, the Polydispersity Index (PDI) is smaller in the turbulent production. In drug delivery applications utilizing lipid-based carriers such as liposome formulations, a PDI of 0.3 or lower is considered acceptable and signifies a homogeneous population

of phospholipid vesicles (Danaei et al., 2018). The lower dimensions and the narrower particle size distribution of the liposomes produced in turbulent conditions, had an impact on the turbidity of the product, which was cleared in the turbulent production.

Table 1. Characteristics of the produced nanoparticles

|           | Laminar | Turbulent |
|-----------|---------|-----------|
| Z-average | 106 nm  | 53 nm     |
| PDI       | 0.32    | 0.28      |
| Turbidity | 930 NTU | 470 NTU   |

#### 4. Conclusions

The coaxial injection mixer shows potential for producing nanoparticles through nanoprecipitation. The vertical configuration is preferred to avoid buoyancy-driven segregation in laminar production. The fluid dynamics regime of the mixer was studied and showed that a turbulent jet is formed at high Flow Momentum Ratio ( $FMR$ ) and Reynolds number ( $N_{Re}$ ). Mixing time was found to depend on both  $FMR$  and  $N_{Re}$  and was modelled using a power law equation. Results showed that the nanoparticles produced in turbulence were smaller and more uniform in size, with a weight-average hydrodynamic diameter half that of those produced in laminar conditions. The improved size uniformity and reduced dimensions of the particles produced in turbulence resulted in a clearer final product. This study suggests that micromixing is a more favourable method for producing liposomes due to improved characteristics and higher productivity compared to interdiffusion. Further studies should be focused to assess the impact of the fluid-dynamic on the encapsulation efficiency and loading of active principles.

#### References

- Bałdyga, J., & Bourne, J. R. (1999). *Turbulent Mixing and Chemical Reactions*. Wiley.
- Bochicchio, S., Dalmoro, A., Lamberti, G., & Barba, A. A. (2020). Advances in Nanoliposomes Production for Ferrous Sulfate Delivery. *Pharmaceutics*, 12(5).
- Carugo, D., Bottaro, E., Owen, J., Stride, E., & Nastruzzi, C. (2016). Liposome production by microfluidics: potential and limiting factors. *Scientific Reports*, 6(1), 25876.
- Danaei, M., Dehghankhold, M., Ataei, S., Hasanzadeh Davarani, F., Javanmard, R., Dokhani, A., . . . Mozafari, M. R. (2018). Impact of Particle Size and Polydispersity Index on the Clinical Applications of Lipidic Nanocarrier Systems. *Pharmaceutics*, 10(2).
- Gobert, S. R. L., Kuhn, S., Braeken, L., & Thomassen, L. C. J. (2017). Characterization of Milli- and Microflow Reactors: Mixing Efficiency and Residence Time Distribution. *Organic Process Research & Development*, 21(4), 531-542.
- Has, C., & Sunthar, P. (2020). A comprehensive review on recent preparation techniques of liposomes. *Journal of Liposome Research*, 30(4), 336-365.
- Iannone, M., Caccavo, D., Barba, A. A., & Lamberti, G. (2022). A low-cost push-pull syringe pump for continuous flow applications. *HardwareX*, 11, e00295.
- Lim, J.-M., Swami, A., Gilson, L. M., Chopra, S., Choi, S., Wu, J., . . . Farokhzad, O. C. (2014). Ultra-High Throughput Synthesis of Nanoparticles with Homogeneous Size Distribution Using a Coaxial Turbulent Jet Mixer. *ACS Nano*, 8(6), 6056-6065.
- Murday, J. S., Siegel, R. W., Stein, J., & Wright, J. F. (2009). Translational nanomedicine: status assessment and opportunities. *Nanomedicine: Nanotechnology, Biology and Medicine*, 5(3), 251-273.
- Paul, E. L., Atiemo-Obeng, V. A., & Kresta, S. M. (2004). *Handbook of Industrial Mixing: Science and Practice*. Wiley.
- Rehage, H., & Kind, M. (2021). The first Damköhler number and its importance for characterizing the influence of mixing on competitive chemical reactions. *Chemical Engineering Science*, 229, 116007.
- Saad, W. S., & Prud'homme, R. K. (2016). Principles of nanoparticle formation by flash nanoprecipitation. *Nano Today*, 11(2), 212-227.
- Usta, M., Ahmad, M. R. C., Pathikonda, G., Khan, I., Gillis, P., Ranjan, D., & Aidun, C. K. C. A. (2023). Coaxial jets with disparate viscosity: mixing and laminarization characteristics. *Journal of Fluid Mechanics*, 955, A43.